Sudden Death of Entanglement Induced by Polarization Mode Dispersion

Cristian Antonelli,[1] Mark Shtaif,[2] and Misha Brodsky[3]

[1]*Dipartimento di Ingegneria Elettrica e dell'Informazione and CNISM, Università dell'Aquila, 67040 L'Aquila, Italy*
[2]*School of Electrical Engineering, Tel-Aviv University, Tel-Aviv 69978, Israel*
[3]*AT&T Labs, 200 Laurel Avenue South, Middletown, New Jersey 07748, USA*
(Received 18 August 2010; revised manuscript received 7 January 2011; published 23 February 2011)

We study the decoherence of polarization-entangled photon pairs subject to the effects of polarization mode dispersion, the chief polarization decoherence mechanism in optical fibers. We show that fiber propagation reveals an intriguing interplay between the concepts of entanglement sudden death, decoherence-free subspaces, and nonlocality. We define the boundaries in which entanglement-based quantum communications protocols relying on fiber propagation can be applied.

DOI: 10.1103/PhysRevLett.106.080404 PACS numbers: 03.65.Ud, 03.65.Yz, 03.67.Hk, 42.50.Ex

Entanglement between particles is a fundamental feature of quantum physics. Just as fundamental is the phenomenon of decoherence that takes place when the entangled quantum system interacts with the environment. One of the most intriguing recent discoveries related to decoherence is the phenomenon of entanglement sudden death (ESD) [1,2]. It manifests itself in an abrupt disappearance of entanglement once the interaction with the environment reaches a certain threshold [3–5]. Beyond the interest that it attracts as a fundamental physical phenomenon, decoherence plays a central role in quantum communications. The security of recent quantum key distribution protocols explicitly relies on the nonlocal properties of entanglement, quantified in terms of the violation of a Bell-type inequality [6–8]. Therefore, establishing the relation between the violation of nonlocality and ESD, which is very interesting from a standpoint of basic physics, has a potentially large impact on the new area of quantum communications.

A configuration that provides an excellent platform for the controlled study of decoherence is that of polarization-entangled photon pairs, distributed over optical fibers. In this scheme the main source of decoherence is the residual optical birefringence randomly accumulating along the fiber. While an alternative entanglement scheme, insensitive to birefringence, has been proposed [9,10], the ease with which light polarization can be manipulated using standard instrumentation leaves polarization entanglement the configuration of choice in many situations [11]. Moreover, numerous sources of polarization-entangled photons suitable for use with standard fibers have recently become available [12]. Hence, understanding the relation between nonlocality and ESD as well as the ultimate limits imposed by fiber birefringence on the distribution of polarization-entangled photons in fibers is a problem of utmost importance.

The fact that optical birefringence is a major polarization decoherence mechanism has been known for a while. Indeed birefringent crystals have been used extensively for the creation and manipulation of special quantum states, such as the maximally entangled mixed states [13,14] or Werner states [13,15]. Similarly, birefringent crystals have also been used for the controlled demonstration of decoherence-free subspaces [16,17]. Yet, the arbitrary birefringence characterizing fiber-optic transmission produces a previously unobserved combination of physical effects.

The accumulation of randomly varying birefringence in fibers leads to a phenomenon known by the name of polarization mode dispersion (PMD) [18]. Since the analysis of the general case of PMD is quite cumbersome, we limit ourselves to the simplest regime of operation in which the optical bandwidth of the photons is small in comparison with the bandwidth over which PMD decorrelates [19]. In this regime, without losing the essence of the problem, the overall effect of PMD resembles that of pure birefringence in the sense that it causes an incident pulse to split into two orthogonally polarized components delayed relative to each other [18]. The polarization states of these two components are known as the principal states of polarization (PSP) and the delay between them is called the differential group delay (DGD).

In contrast to the controlled environment of [13–17], both the PSP and the DGD of real fibers vary stochastically in time. Since typical time constants characterizing the decorrelation of PMD in optical fibers are as long as hours, days, and sometimes months [20], PMD evolution can be considered adiabatic in the context of quantum communications protocols. Thus the density matrix describing the quantum state needs to be evaluated as a function of the arbitrary values of the instantaneous PMD. As a consequence, the parameters of interest obtained from the so-evaluated density matrix are also PMD dependent. The temporal statistics for those parameters could be in principle determined by application of the proper PMD statistics. An approach, in which the randomness of PMD is accounted for in the density matrix itself [21], implicitly assumes ultrafast PMD dynamics and leads to fundamentally different results. This previously unstudied reality produces important consequences to the dynamics of decoherence between polarization-entangled photons.

In this Letter we formulate a quantitative approach to studying PMD-induced disentanglement. We consider the evolution of an arbitrary two-photon state maximally entangled in polarization as each photon propagates through a fiber with PMD. Our studies demonstrate that the unequal and increasing differential delays in both arms always lead to entanglement sudden death [1,2] for all but two special PSPs orientations. That is, our channel causes an abrupt drop to zero in concurrence while a single-photon subjected to the same environment depolarizes asymptotically. Contrary to that, when both delays are sufficiently close in value there exists a range of PSP orientations for which concurrence does not vanish. This is related to the existence of decoherence-free subspaces and offers an opportunity for nonlocal PMD compensation. Finally, when only one photon experiences PMD, the concurrence decays gradually for every PSP orientation. Besides concurrence, we calculate the S parameter of the Clauser-Horne-Shimony-Holt Bell's inequality. Comparing the loss of entanglement (concurrence $C = 0$) and violation of locality ($S > 2$) we discover an intriguing empirical relation between them.

We assume a source in which a pair of polarization-entangled photons is generated either via spontaneous parametric down conversion [22], or by using four-wave mixing [23,24]. In either case, the quantum state of the generated photon pair can be expressed as

$$|\psi\rangle = \int \frac{d\omega}{2\pi} \tilde{f}(\omega)|\omega, -\omega\rangle \otimes \frac{|\underline{u}_A, \underline{u}_B\rangle + e^{i\alpha}|\underline{u}'_A, \underline{u}'_B\rangle}{\sqrt{2}}, \quad (1)$$

where the left-hand side of the tensor product represents the frequency waveform, whereas the right-hand side represents polarization modes. The frequency variable ω denotes the offset from the central frequency, which is equal to the pump frequency in sources relying on four-wave mixing and to half the pump frequency in sources based on spontaneous parametric down conversion. The function $\tilde{f}(\omega)$ represents the effect of phase matching as well as the possible effects of filters, as we shall see below. Notice that normalization of the state $|\psi\rangle$ implies that $\int d\omega |\tilde{f}(\omega)|^2 = 2\pi T^{-1}$, with T being the integration time of the detectors used in the setup. In what follows, the state (1) will be referred to as the input state of the system, which consists of the two optical paths that lead the entangled photons from the source of entanglement towards its users, conventionally referred to as Alice and Bob. The terms $\underline{u}_{A,B}$ and $\underline{u}'_{A,B}$ are the Jones vectors that correspond to the excited polarization states of Alice's and Bob's photons, respectively. We use primes to denote orthogonality in polarization space, so that $\underline{u}_{A,B} \cdot \underline{u}'_{A,B} = 0$. The phase factor α is introduced for consistency with the experimental generation of polarization-entangled photon pairs [23]. Notice that the frequency dependent part in (1) can be reexpressed as

$$\int \frac{d\omega}{2\pi} \tilde{f}(\omega)|\omega, -\omega\rangle = \iint dt_A dt_B f(t_A - t_B)|t_A, t_B\rangle, \quad (2)$$

with $f(\tau)$ being the inverse Fourier transform of $\tilde{f}(\omega)$. As can be deduced from the form of Eq. (2), $|f(\tau)|^2$ is proportional to the probability density function that Bob's photon precedes Alice's photon (or vice versa) by τ. For brevity, we will denote the polarization dependent part in the tensor product (1) by $|\psi_p\rangle = [|\underline{u}_A, \underline{u}_B\rangle + e^{i\alpha}|\underline{u}'_A, \underline{u}'_B\rangle]/\sqrt{2}$, whereas the expression in Eq. (2) will be shortly denoted as $|f(t_A - t_B)\rangle$. The overall state is then expressed as $|\psi\rangle = |f(t_A - t_B)\rangle \otimes |\psi_p\rangle$.

Let us now represent the state $|\psi\rangle$ in terms of the principal states of the PMD in the two arms. We denote by $\{\underline{s}_A, \underline{s}'_A\}$ and $\{\underline{s}_B, \underline{s}'_B\}$ the pairs of Jones vectors that correspond to the PSP along the paths of photons A and B, respectively. We now represent $|\psi_p\rangle$ in the basis of the PSP modes as follows:

$$|\psi_p\rangle = \eta_1(|\underline{s}_A, \underline{s}_B\rangle + e^{i\tilde{\alpha}_1}|\underline{s}'_A, \underline{s}'_B\rangle)/\sqrt{2} + \eta_2(|\underline{s}_A, \underline{s}'_B\rangle - e^{i\tilde{\alpha}_2}|\underline{s}'_A, \underline{s}_B\rangle)/\sqrt{2}, \quad (3)$$

where the coefficients η_1 and η_2 are given by

$$\eta_1 = (\underline{s}_A \cdot \underline{u}_A)(\underline{s}_B \cdot \underline{u}_B) + e^{i\alpha}(\underline{s}_A \cdot \underline{u}'_A)(\underline{s}_B \cdot \underline{u}'_B), \quad (4)$$

$$\eta_2 = (\underline{s}_A \cdot \underline{u}_A)(\underline{s}'_B \cdot \underline{u}_B) + e^{i\alpha}(\underline{s}_A \cdot \underline{u}'_A)(\underline{s}'_B \cdot \underline{u}'_B), \quad (5)$$

and where $\tilde{\alpha}_i$ is defined through the relation $\eta_i = |\eta_i| \exp(i(\alpha - \tilde{\alpha}_i)/2)$. Also, note that, as is implied by state normalization, $|\eta_1|^2 + |\eta_2|^2 = 1$. The quantity $|\eta_1|^2$ is related to the alignment between the input two-photon state (1) and the PSP. Thus, for example, in the case of $\underline{u}_A = \underline{s}_A$ and $\underline{u}_B = \underline{s}_B$, the value of $|\eta_1|^2$ is unity. In the presence of PMD the arrival time of the A photon is delayed by $\tau_A/2$ in the $\underline{s}_A$ polarization and advanced by the same amount in the $\underline{s}'_A$ polarization, and the B photon undergoes a similar process. Therefore, the output state, i.e., the two-photon state after propagating through media with PMD, can be expressed as

$$\begin{aligned}|\psi_{\text{out}}\rangle = &\frac{\eta_1}{\sqrt{2}}\left|f\left(t_A - t_B - \frac{\tau_A - \tau_B}{2}\right)\right\rangle \otimes |\underline{s}_A, \underline{s}_B\rangle \\ &+ \frac{\eta_2}{\sqrt{2}}\left|f\left(t_A - t_B - \frac{\tau_A + \tau_B}{2}\right)\right\rangle \otimes |\underline{s}_A, \underline{s}'_B\rangle \\ &- \frac{\eta_2^* e^{i\tilde{\alpha}_2}}{\sqrt{2}}\left|f\left(t_A - t_B + \frac{\tau_A + \tau_B}{2}\right)\right\rangle \otimes |\underline{s}'_A, \underline{s}_B\rangle \\ &+ \frac{\eta_1^* e^{i\tilde{\alpha}_1}}{\sqrt{2}}\left|f\left(t_A - t_B + \frac{\tau_A - \tau_B}{2}\right)\right\rangle \otimes |\underline{s}'_A, \underline{s}'_B\rangle. \quad (6)\end{aligned}$$

The density matrix that characterizes the detected field is given by $\rho = \int dt'_A dt'_B \langle t'_A, t'_B|\psi_{\text{out}}\rangle\langle\psi_{\text{out}}|t'_A, t'_B\rangle$, where tracing over the time modes is performed in order to account for the fact that the photo-detection process is not sensitive to the photon's time of arrival (within the detector's integration window). The elements of the resulting density matrix, establishing the correspondence

$(\underline{s}_A, \underline{s}_B) \leftrightarrow 1$, $(\underline{s}'_A, \underline{s}_B) \leftrightarrow 2$, $(\underline{s}_A, \underline{s}'_B) \leftrightarrow 3$, and $(\underline{s}'_A, \underline{s}'_B) \leftrightarrow 4$ are then given by

$$\begin{aligned}
&\rho_{11} = \rho_{44} = |\eta_1|^2/2, \qquad \rho_{22} = \rho_{33} = |\eta_2|^2/2,\\
&\rho_{31} = -\rho_{42} = \eta_1^* \eta_2 R_f(\tau_B)/2,\\
&\rho_{21} = -\rho_{43} = -\eta_1^* \eta_2^* e^{i\alpha} R_f(\tau_A)/2,\\
&\rho_{41} = (\eta_1^*)^2 e^{i\alpha} R_f(\tau_A - \tau_B)/2,\\
&\rho_{23} = -(\eta_2^*)^2 e^{i\alpha} R_f(\tau_A + \tau_B)/2,
\end{aligned} \tag{7}$$

where $R_f(\tau) = T \int dt f^*(t) f(t+\tau)$ is the autocorrelation function of $f(t)$, normalized such that $R_f(0) = 1$. The function $\tilde{f}(\omega)$ which defines the frequency contents of the two generated photons accounts for the phase-matching spectrum, as well as for filtering applied to the two generated photons. In this case $\tilde{f}(\omega) = \tilde{f}_{\rm pm}(\omega) H_A(\omega) H_B(-\omega)$, where $H_A(\omega)$ and $H_B(\omega)$ denote the transfer functions of Alice's and Bob's filters, respectively, and where $\tilde{f}_{\rm pm}(\omega)$ represents the phase-matching spectrum. In most applications, the filters are much narrower than the phase-matching spectrum, in which case $\tilde{f}_{\rm pm}(\omega)$ can be replaced by a constant, such that $\tilde{f}(\omega) \propto H_A(\omega) H_B(-\omega)$. Notice that the effect of PMD scales with the width of the autocorrelation function $R_f(\tau)$, which is in turn determined by the overlap bandwidth of Alice's and Bob's filters, namely, by the width of $|H_A(\omega) H_B(-\omega)|^2$. For illustrative purposes, in all the numerical examples considered in what follows, we will assume that $|H_A(\omega)|^2$ and $|H_B(\omega)|^2$ are Gaussian functions of root mean square bandwidth B and central frequencies ω_A and $\omega_B = -\omega_A$, respectively.

We now turn to the characterization of the degree of entanglement of the PMD-affected two-photon state. In the presence of PMD, tracing over the time of arrival puts the system in a partially mixed state. The extent of this process can be quantified with the help of several proposed entanglement metrics [25–27]. We choose to calculate purity, concurrence [27], and Bell's S parameter, thus assessing the largest possible violation of Bell's inequality in the Clauser-Horne-Shimony-Holt (CHSH) definition [28]. Because the individual photon states are maximally mixed, the two-photon density matrix can be reduced to a Bell-diagonal form by a proper change of basis [29]. This enables a fully analytical evaluation of C and S. Note that a Bell-diagonal matrix is defined by three real parameters only. In the case of PMD they are τ_A, τ_B, and $|\eta_1|^2$ and the functional dependence of C and S on them is given in [29].

In the simplest case of PMD present in only one of the two fibers, as described, for example, by $\tau_B = 0$, the concurrence is given by $C = |R_f(\tau_A)|$; in this case the concurrence is independent of the PSP orientation and can only decay asymptotically with τ_A. Correspondingly, the S parameter acquires the maximum value compatible with such concurrence, that is $S = 2\sqrt{1 + C^2}$ [30], indicating unconditional violation of Bell's inequality. Note that the two cases $|\eta_1| = 1$ and $|\eta_1| = 0$, where concurrence simplifies to $C = |R_f(\tau_A - \tau_B)|$ and $C = |R_f(\tau_A + \tau_B)|$, respectively, are equivalent to that of single-arm PMD, with corresponding nonzero DGDs equal to $\tau_A - \tau_B$ and $\tau_A + \tau_B$. Remarkably, for $\tau_A = \tau_B$ and $|\eta_1| = 1$, the concurrence is unity, regardless of the DGD magnitude. This result is quite interesting and it is directly related to the concept of decoherence-free subspaces [16,17]. In this situation the output state, when expressed in the basis of the PSP, is a superposition of a state in which both photons are delayed, with a state in which they are both advanced [see Eq. (3)], such that they reach the detectors simultaneously. Since in this state, knowledge of the photon's times of arrival discloses no information on their polarization states, tracing out time involves no loss of information. Decoherence-free subspaces would not be allowed if PMD dynamics were fast on the scale of measurements, as assumed in [21].

The dependence of the two-photon state decoherence on the PMD parameters in the general case is more cumbersome, as it is governed by the two DGD values τ_A and τ_B and by the PSP orientation, accounted for by $|\eta_1|$. For illustrative purposes, we plot in Fig. 1 the concurrence as a function of τ_A (normalized to B^{-1}) and $|\eta_1|^2$ for two different settings of τ_B, so as to describe PMD effects for the most relevant realizations of PMD parameters. In Fig. 1(a) we plot the concurrence for the case of identical DGDs, $\tau_B = \tau_A$, whereas in Fig. 1(b) the value of τ_B is fixed and equal to $1.7B^{-1}$. The range of values for which entanglement disappears entirely (i.e., $C = 0$) is represented by the flat part of the surface (red color online). The rest of the surface (green color online) corresponds to settings in which entanglement exists (i.e., $C > 0$), with $S > 2$ in the lighter shaded region, and $S \leq 2$ in the darker shaded region. In the case where the DGD values are equal [Fig. 1(a)], the concurrence approaches unity when $|\eta_1|^2 \to 1$. That is because in this situation the input state is given by the first term in Eq. (3), and it is not affected by the loss of time of arrival information. In the opposite limit, when $|\eta_1| = 0$, the concurrence is given by $C = |R_f(2\tau_A)|$ and reduces towards zero asymptotically for large DGD values. Figure 1(b) also illustrates that concurrence can be unity only when the DGD values in the two arms are equal.

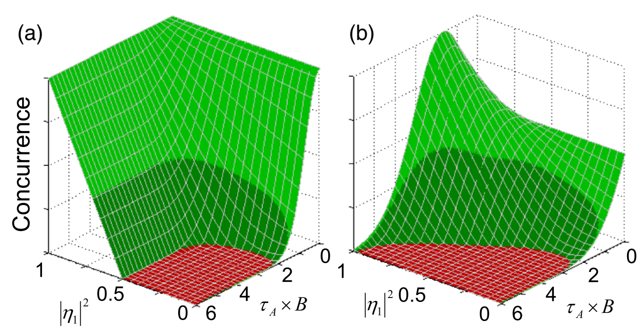

FIG. 1 (color online). Concurrence versus τ_A and $|\eta_1|^2$. In (a) $\tau_B = \tau_A$, whereas in (b) $\tau_B \simeq 1.7B^{-1}$. Lighter shaded (light green online): $S > 2$. Darker shaded (dark green online): $S < 2$. Flat region (red online): $C = 0$ and $S < 2$.

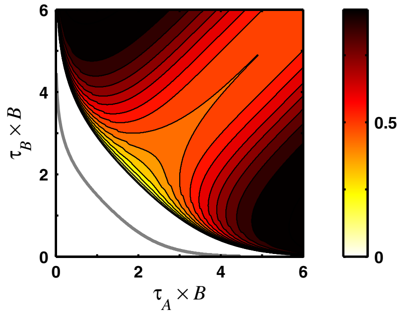

FIG. 2 (color online). ESD probability (see text) versus τ_A and τ_B normalized to B^{-1}. The gray line is the boundary $S = 2$. Below and to the left of the gray line $S > 2$ for all values of $|\eta_1|^2$, whereas to its right $S < 2$ for some range of $|\eta_1|^2$.

The most interesting feature in Fig. 1 is the abrupt transition of the concurrence to zero when either τ_A or $|\eta_1|^2$ are varied continuously. The abrupt decay of concurrence is contrasted with the asymptotic decoherence that would be experienced by a single photon if it evolved in the same environment. Indeed, the purity of a polarized single-photon pulse characterized by a Jones vector $\underline{u}$ and a time-mode distribution $g(t)$, transmitted through a fiber with DGD τ and PSP $\underline{s}$, is given by $p = 1 - 2|\underline{u} \cdot \underline{s}|^2 (1 - |\underline{u} \cdot \underline{s}|^2)[1 - |R_g(\tau)|^2]$, with $R_g(\tau)$ the autocorrelation function of $g(t)$. This is a manifestation of the entanglement sudden death (ESD) that has been previously reported in other physical systems [1–5].

In general, PSP orientation in optical fibers varies faster than the DGD, resulting in a uniform distribution of the parameter $|\eta_1|^2$ between 0 and 1. For each given combination of τ_A and τ_B, we evaluate the fraction of the interval between 0 and 1 in which ESD occurs. This quantity, which can be interpreted as the probability of ESD (conditioned on the DGD values) is illustrated in Fig. 2. Note the existence of a completely white region that shows the range of DGD values in which entanglement does not disappear for any value of $|\eta_1|^2$. In contrast to that, the darker tones mark areas for which ESD occurs for some range of $|\eta_1|^2$. The color progressively turns dark for highly differing DGD values. On the other hand, when increasing DGDs remain nearly equal, the probability of ESD is about 0.5 [29].

Many applications involving entanglement rely directly on the violation of Bell's inequality [7,8] and, therefore, we compute the maximum value of the CHSH S—parameter [28] for the density matrix Eq. (7) [31]. In Fig. 1, the range of parameters in which $S > 2$—meaning that the CHSH inequality is violated—is represented by the lighter shaded part of the surface, whereas the darker shaded part of the surface represents states in which $C > 0$, but there is no violation of the CHSH inequality ($S \leq 2$). The thick gray line in Fig. 2 also marks the $S = 2$ boundary. Below and to the left of this line $S > 2$ for all $|\eta_1|^2$ values, but to its right S may be smaller than 2 for some relative PSP orientations. Intriguingly, this nonlocality boundary (thick gray line) nearly perfectly reproduces the boundary to the ESD-free region (the white area) if the scale on both axes is stretched by a factor of 1.5.

To conclude, we have carried out what we believe to be the first quantitative analysis of the decoherence of polarization-entangled photons propagating in optical fibers. Our study shows that PMD leads to entanglement sudden death in all but a well-defined restricted set of realizations of fiber birefringence. In addition, we demonstrated how decoherence-free subspaces can be reached via nonlocal PMD compensation. The ultimate limits imposed by fiber birefringence to applications based on nonlocal properties of polarization entanglement were shown to be intriguingly related with the phenomenon of entanglement sudden death.

[1] J. H. Eberly and T. Yu, Science **316**, 555 (2007).
[2] T. Yu and J. H. Eberly, Science **323**, 598 (2009).
[3] M. P. Almeida *et al.*, Science **316**, 579 (2007).
[4] J. Laurat *et al.*, Phys. Rev. Lett. **99**, 180504 (2007).
[5] K. Ann and G. Jaeger, Found. Phys. **39**, 790 (2009).
[6] A. K. Ekert, Phys. Rev. Lett. **67**, 661 (1991).
[7] A. Acin, S. Massar, and S. Pironio, New J. Phys. **8**, 126 (2006).
[8] A. Acin *et al.*, Phys. Rev. Lett. **98**, 230501 (2007).
[9] R. T. Thew *et al.*, Phys. Rev. A **66**, 062304 (2002).
[10] S. Tanzilli *et al.*, Eur. Phys. J. D **18**, 155 (2002).
[11] A. Poppe *et al.*, Opt. Express **12**, 3865 (2004); Hübel *et al.*, Opt. Express **15**, 7853 (2007).
[12] S. X. Wang and G. S. Kanter, IEEE J. Sel. Top. Quantum Electron. **15**, 1733 (2009).
[13] M. Barbieri *et al.*, Phys. Rev. Lett. **92**, 177901 (2004).
[14] N. A. Peters *et al.*, Phys. Rev. Lett. **92**, 133601 (2004).
[15] A. G. White *et al.*, Phys. Rev. A **65**, 012301 (2001).
[16] P. G. Kwiat *et al.*, Science **290**, 498 (2000).
[17] J. B. Altepeter *et al.*, Phys. Rev. Lett. **92**, 147901 (2004).
[18] J. P. Gordon and H. Kogelnik, Proc. Natl. Acad. Sci. U.S.A. **97**, 4541 (2000).
[19] M. Shtaif and A. Mecozzi, Opt. Lett. **25**, 707 (2000).
[20] M. Brodsky *et al.*, J. Lightwave Technol. **24**, 4584 (2006).
[21] P. S. Y. Poon and C. K. Law, Phys. Rev. A **77**, 032330 (2008).
[22] D. C. Burnham and D. L. Weinberg, Phys. Rev. Lett. **25**, 84 (1970).
[23] X. Li *et al.*, Opt. Express **12**, 3737 (2004).
[24] H. Takesue and K. Inoue, Phys. Rev. A **70**, 031802 (2004).
[25] G. S. Jaeger *et al.*, Phys. Rev. A **67**, 032307 (2003).
[26] R. Horodecky *et al.*, Rev. Mod. Phys. **81**, 865 (2009).
[27] W. K. Wootters, Phys. Rev. Lett. **80**, 2245 (1998).
[28] J. F. Clauser, M. A. Horne, A. Shimony, and R. A. Holt, Phys. Rev. Lett. **23**, 880 (1969).
[29] See supplemental material at http://link.aps.org/supplemental/10.1103/PhysRevLett.106.080404 for analytical expressions for concurrence and S parameter.
[30] F. Verstraete and M. M. Wolf, Phys. Rev. Lett. **89**, 170401 (2002).
[31] R. Horodecki, P. Horodecki, and M. Horodecki, Phys. Lett. A **200**, 340 (1995).